Cancer Research

A Simple Approach to Cancer Therapy Afforded by Multivalent Pseudopeptides That Target Cell-Surface Nucleoproteins

Damien Destouches[1,2], Nicolas Page[3], Yamina Hamma-Kourbali[1], Valérie Machi[3], Olivier Chaloin[3], Sophie Frechault[1], Charalampos Birmpas[7], Panagiotis Katsoris[7], Julien Beyrath[3], Patricia Albanese[1], Marie Maurer[6], Gilles Carpentier[1], Jean-Marc Strub[5], Alain Van Dorsselaer[5], Sylviane Muller[3], Dominique Bagnard[4], Jean Paul Briand[3], and José Courty[1]

Abstract

Recent studies have implicated the involvement of cell surface forms of nucleolin in tumor growth. In this study, we investigated whether a synthetic ligand of cell-surface nucleolin known as N6L could exert antitumor activity. We found that N6L inhibits the anchorage-dependent and independent growth of tumor cell lines and that it also hampers angiogenesis. Additionally, we found that N6L is a proapoptotic molecule that increases Annexin V staining and caspase-3/7 activity *in vitro* and DNA fragmentation *in vivo*. Through affinity isolation experiments and mass-spectrometry analysis, we also identified nucleophosmin as a new N6L target. Notably, in mouse xenograft models, N6L administration inhibited human tumor growth. Biodistribution studies carried out in tumor-bearing mice indicated that following administration N6L rapidly localizes to tumor tissue, consistent with its observed antitumor effects. Our findings define N6L as a novel anticancer drug candidate warranting further investigation. *Cancer Res; 71(9); 3296–305. ©2011 AACR.*

Introduction

Surface nucleolin expression is enhanced in various tumor cell lines and in activated endothelial cells (1–4). Furthermore, several molecules related to cell proliferation or cell differentiation have been reported to be ligands for cell-surface nucleolin. Among these molecules are hepatocyte growth factor, pleotrophin, and midkine, all of which play important roles in tumor development (5–8). In addition, molecules such as urokinase, which are involved in mechanisms regulating pericellular proteolysis and cell-surface adhesion mitogenesis, bind and are cointernalized along with cell-surface nucleolin (9, 10). Other cell-surface nucleolin binding proteins, such as laminin-1, factor J, and L- and P-selectins, are involved in cell differentiation, cell adhesion regulation, leukocyte trafficking, inflammation, and angiogenesis (11–14). Cell-surface nucleolin has been validated as a novel target for anticancer therapy by using several molecules such as endostatin, the AS1411 aptamer, acharan sulfate, the F3 tumor-homing peptide coupled to radioactive isotopes (15–17), and the HB-19 pseudopeptide (18). Furthermore, targeting nucleolin with a specific antibody results in the activation of endothelial cell apoptosis by decreasing antiapoptotic Bcl-2 mRNA in the tumor vasculature (19).

In addition to its functions at the cell surface, nucleolin plays a critical role in the apoptotic process in which it regulates fundamental proteins such as Bcl-2, p53, and retinoblastoma. In chronic B-cell leukemia cells, overexpression of nucleolin has been directly linked to Bcl-2 mRNA stabilization, leading to apoptosis blockade and resistance (20, 21). In MCF-7 breast carcinoma cells and HeLa cells, a decrease in nucleolin level leads to an increase in p53 and apoptosis (22, 23). Nucleolin associates with tumor suppressor retinoblastoma protein, leading to cancer cell transformation (24).

In this study, we have investigated the antitumor activities, the mechanism of action, and the biodistribution in mice bearing human xenograft tumors of a synthetic ligand of cell-surface nucleolin known as N6L. In addition, using affinity isolation experiments and mass-spectrometry analysis, we identified other N6L molecular partners.

Authors' Affiliations: [1]Laboratoire de Recherche sur la Croissance Cellulaire, la Réparation et la Régénération Tissulaires (CRRET), CNRS, Université Paris-Est, Créteil; [2]ImmuPharma, Mulhouse; [3]CNRS, Immunologie et Chimie Thérapeutiques, Institut de Biologie Moléculaire et Cellulaire, Strasbourg; [4]INSERM U682 and [5]CNRS, Laboratoire de Spectrométrie de Masse BioOrganique, Université de Strasbourg, Strasbourg; [6]Génétique fonctionnelle et médicale UMR 955 INRA, École Nationale Vétérinaire d'Alfort, Maisons-Alfort, France; and [7]Division of Genetics, Cell and Development Biology, Department of Biology, University of Patras, Patras, Greece

Note: Supplementary data for this article are available at Cancer Research Online (http://cancerres.aacrjournals.org/).

D. Destouches and N. Page contributed equally to this work.

Corresponding Author: Jose Courty, University Paris EST, 61 avenue du General de Gaulle, Creteil 94010, France. Phone: 0145-171797; Fax: 0145-171816; E-mail: courty@univ-paris12.fr

doi: 10.1158/0008-5472.CAN-10-3459

Materials and Methods

Peptide constructs

Synthesis of N4L, N5L, N6L, and N8L is described in detail in Supplementary Methods; briefly, the lysine-rich template is a 3_{10} helical matrix composed respectively of 4, 5, 6, and 8 repeats of Lys-Aib-Gly, the pseudotripeptides Lys[CH_2N]Pro-Arg being grafted onto the ε NH_2 of the matrix Lys residues. Fluorescent conjugates were prepared starting from the N6L-Cys derivative. The various conjugates were then purified by high-performance liquid chromatography and lyophilized.

Cell growth and toxicity assays

Cell growth was carried out as previously described (18) and cell viability measured and quantified by Cell Titer Aqueous One (MTS assay) according to the manufacturer's instructions.

Chicken embryo chorioallantoic membrane assay

Chorioallantoic membrane (CAM) assay was carried out as previously described (18).

Tumor cell xenograft in nude mice

Experiments with human solid tumor xenografts in nude mice were carried out as previously described (18). For lymphoma experiments, A20 (5×10^6) or T29 lymphoma (5×10^5) was injected into BALB/c and C57BL/6 mouse tail vein after irradiation at 3.5 Gy/mice. Five days later, mice were randomly separated into 2 groups and treated with NaCl 0.9% (control group) or N6L 8 mg/kg 5 times per week by i.p. injection. All *in vivo* experiments were carried out with the approval of the appropriate ethical committee and under conditions established by the European Union.

In vivo tumor targeting of N6L

N6L-alexa fluor 633 (100 μg/mouse) was injected through the tail vein into nude mice bearing MDA-MB 231 xenograft tumors. Images were taken using the NightOwl Bioimager (Berthold Technologies). Signal intensity was evaluated using WinLight32 software.

Tissue preparation and apoptosis assay

Immediately after surgical resection, MDA-MB 231 tumors were frozen in liquid nitrogen and stored at −80°C. Fragmented DNA was stained using the ApopTag Isol Dual Fluorescent kit according to the manufacturer's instructions (Millipore). Positive terminal deoxynucleotidyl transferase–mediated dUTP nick end labeling (TUNEL) cells were automatically counted by a program detecting the maximum of Sobel's gradients, as previously described (25).

In vitro apoptosis assays

Cell death occurring in the presence of the N6L peptide was measured on a time scale of 30 minutes to 24 hours. Briefly, treated cells were harvested, rinsed, and resuspended in Annexin V-binding buffer containing allophycocyanin (APC)-labeled Annexin V (BD Bioscience) and propidium iodide (PI). Samples were analyzed using a FACSCalibur flow cytometer (BD Biosciences). The decrease in the mitochondrial transmembrane potential was detected by the reduction of DiOC6 (3) dye uptake, and caspase-3/7 activity was measured using the Caspase-Glo 3/7 detection assay kit according to the manufacturer's instruction (Promega).

Immunofluorescence staining and ApoTome microscopy

For immunofluorescence assays, after adding N6L-alexa fluor 488 0.5 μmol/L at 37°C for 30 minutes, cells were washed and fixed with cold acetone at −20°C for 10 minutes or with paraformaldehyde (PFA) 4% at room temperature for 10 minutes. Nucleolin and nucleophosmin were revealed using antinucleolin (MS-3, Santa Cruz Biotechnologies) and anti-nucleophosmin (Abcam) antibodies. DAPI 1 μg/mL was used for nuclear staining. All slides were observed with an AxioObserver Z.1 microscope equipped with an ApoTome system of structured illumination (Zeiss).

Short interfering RNA transfection

MDA-MB 435 cells were plated in 6 wells-plates and incubated for 24 hours at 37°C. Cells were then transfected at a final concentration of 100 nmol/L short interfering RNA (siRNA) using Lipofectamine 2,000 reagent (Invitrogen) according to the manufacturer's instructions. Nucleolin and nucleophosmin siRNA were purchased from Abnova, and GFP siRNA was purchased from Ambion.

Surface plasmon resonance analysis

All binding experiments were conducted using the BIACORE 3000 system and are described in detail in Supplementary Methods.

Statistical analysis

Statistical significance was determined by the ANOVA unpaired *t* test, using GraphPad Prism 4.0 software. Values of $P < 0.05$ were considered significant. Comparisons of survival curves were made using the Kaplan–Meier product-limit method and analysis by the log rank test. Statistical significance was defined as $P < 0.05$.

Results

Effect of N6L on tumor and endothelial cell survival and proliferation

We generated multivalent pseudopeptide analogues for use in exploring the most efficient size and shape of the template and the optimal number of grafted pseudotripeptides Lys[CH_2N]Pro-Arg. We then investigated the effects of these compounds on cell growth, using T29 cells. Comparative studies indicated that the optimum inhibitory effect was achieved with N6L (Fig. 1A). No effect of N6L was observed on the viability of BALB/c mouse lymph node cells used as a control (data not shown). N6L is built on a lysine-rich helicoid template formed by a repeat of 6 tripeptide units, (Lys-Aib-Gly), the pseudotripeptides Lys[CH_2N]Pro-Arg being bound to the Lys εNH_2 groups of the template (Fig. 1B).

We then investigated the effect of N6L in a soft-agar colony-forming assay. In all cases, colony formation was reduced by

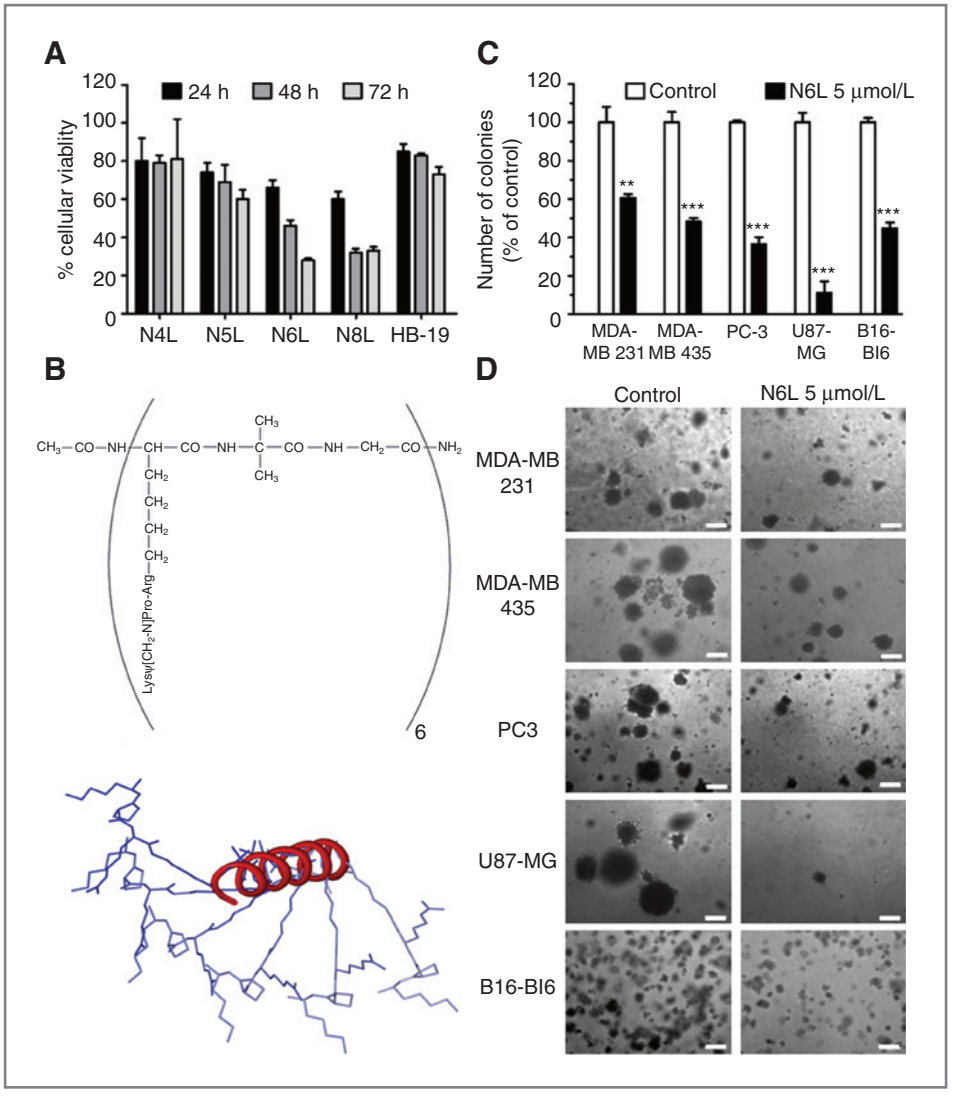

Figure 1. N6L exerts growth-inhibitory activity on various tumor cells. A, effect of N6L on T29 cell growth. Cells were cultured for 24, 48, or 72 hours with 20 μmol/L of N4L, N5L, N6L, N8L, or HB-19. Data are expressed as percentage of cell survival compared to the control (untreated cells). Means ± SD ($n = 3$). B, representation of semideveloped formula and 3D structure of N6L. N6L is built on a 3_{10} helical matrix composed of 6 repeats of Lys-Aib-Gly. Six reduced peptide bond pseudotripeptides Lys[CH2N]-Pro-Arg are grafted onto the ε lysine residues of the matrix. C, N6L inhibits colony formation of various tumor cell lines in soft agar assay. Cells were treated every 2 days with the indicated pseudopeptides used at 5 μmol/L for 10 to 21 days. D, representative pictures of colonies formed by various tumor cell lines treated or not with 5 μmol/L of N6L. Scale bars represent 200 μm.

50% or more, except for MDA-MB 231, in which 40% inhibition was observed (Fig. 1C and D).

Whatever the type of tumor cell, cell growth was significantly inhibited by N6L, with an inhibition of cell growth (GI_{50}) value ranging from 5 to more than 40 μmol/L (Table 1). In addition, N6L significantly inhibited growth of human umbilical vein endothelial cells (HUVEC), with a 60% reduction at 10 μmol/L N6L (Fig. 2A). No effect was observed in cells treated with highly basic compounds such as polyarginine. In *in vivo* angiogenic assay, addition of N6L impaired the branching of newly formed blood vessels in comparison with the PBS control (Fig. 2B). Quantitative analysis indicated that the maximal inhibition of angiogenesis was reached with the application of 400 pmol of N6L.

Antitumor effect of the multivalent pseudopeptide N6L

To determine the *in vivo* efficacy of N6L as an antitumor molecule, we carried out several experiments with mice bearing human xenograft tumors and murine lymphoma. Compared with the control, N6L induced significant inhibition of tumor growth in mice grafted with MDA-MB 231 or PC3 cells. Indeed, N6L used at concentrations as low as 1 mg/kg inhibited tumor growth up to 90% ($P < 0.001$) and 40% for MDA-MB 231 and PC3 cells, respectively (Fig. 2C and D). It is worth mentioning that N6L efficacy on MDA-MB 231 is optimal between low and high doses, which may reveal a biphasic dose response as already observed for other regulators of cell growth (26).

Similar results were obtained by analyzing the weights of tumors harvested from tumor-bearing mice (Supplementary Fig. S1). Consistent with *in vitro* observations (Table 1), the survival of N6L-treated mice bearing A20 and T29 lymphomas was significantly prolonged compared with controls (Fig. 2E and F). We found no apparent toxicity in several organs of N6L-treated mice and did not observe significant changes in their body weight compared with control mice (data not shown). These results indicate that

Table 1. Activity of N6L pseudopeptide against a range of tumor cell lines studied by MTS bioassay

Cell line	Tumor cell origin	N6L GI_{50}, μmol/L
T29	Murine T-cell lymphoma	10.7 ± 1.8
MOLT-4	Acute lymphoblastic leukemia	38.4 ± 2.3
Jurkat	Acute T-cell leukemia	33.4 ± 1.3
A20	Murine B-cell lymphoma	5 ± 2.5
RAJI	Burkitt lymphoma	5.8 ± 0.4
HL-60	Acute promyelocytic leukemia	15.3 ± 5.5
HL-60 MX2	Acute promyelocytic leukemia MX resistant	26 ± 6.5
RAW	Monocyte/macrophage cell line from mouse	14 ± 0.4
HCT116	Colorectal carcinoma	34 ± 6
HCT116 $p53^{-/-}$	Colorectal carcinoma $p53^{-/-}$	32 ± 8
MDA-MB 231	Mammary gland adenocarcinoma	20 ± 2.4
MDA-MB 435	Melanoma	7.7 ± 1.2
B16-Bl6	Murine melanoma	24.6 ± 3.5
U87-MG	Glioblastoma	25.1 ± 3.9
U373-MG	Glioblastoma	6.7 ± 2.0
Renca	Renal carcinoma	>40

NOTE: GI_{50} ± SD values of at least 2 independent experiments for each cell line are shown. Cells are treated with N6L over a period of 72 hours.

N6L effectively reduced tumor growth in mice without evidence of toxicity.

Identification of N6L cell targets

To identify molecular targets of N6L, we undertook a series of affinity isolation experiments based on a previously described method (27) using Raji and MDA-MB 231 cells and biotin-labeled N6L. Affinity isolated proteins were subjected to SDS-PAGE and analyzed by mass spectrometry (Supplementary Table S1). This procedure enabled us to identify several proteins involved in a ribonucleoproteic complex, including nucleolin and nucleophosmin (Fig. 3A). This result was validated by Western blot experiments (Fig. 3B). Analysis of the equilibrium binding parameters using surface plasmon resonance experiments indicated that both nucleolin and nucleophosmin bound to N6L in a dose-dependent manner (Fig. 3C). The interaction of nucleolin and nucleophosmin with N6L was deemed to be monophasic with an affinity constant of 0.5 and 1 nmol/L, respectively. In contrast, no binding was observed either with ribosomal L5 protein used as a control (Fig. 3C) or with HSC70 and glutathione *S*-transferase proteins (data not shown). Moreover, considering that nucleolin and nucleophosmin are usually found to be associated with RNA in the ribosome biogenesis pathway, we investigated whether the interaction between nucleolin or nucleophosmin and N6L is direct or dependent on a bridging molecule like RNA. Treatment of the affinity isolated fraction with a large excess of RNAse revealed that nucleolin—but not nucleophosmin—interactions with N6L were RNA-mediated (Fig. 3B). This indicated that, whereas N6L is able to interact with both nucleolin and nucleophosmin, RNA could modulate nucleolin structure to promote N6L binding to nucleolin. These results are reinforced by data from cell-surface biotinylation experiments which provided evidence on the presence of nucleophosmin and nucleolin at the tumor cell surface (Fig. 3D), as well as on the colocalization of N6L with nucleophosmin in nonpermeabilized MDA-MB 231 cells (Fig. 3E).

N6L is translocated into the nucleolus

We used N6L conjugated with various fluorescent reagents to study its cell trafficking. Fluorescent peptides appeared in both the cytoplasm and the nucleus (Fig. 4A). Addition of 100-fold molar excess of unlabeled N6L completely abolished staining, demonstrating the specificity of the signal (Fig. 4B). Double-immunofluorescent staining with antinucleolin antibody and N6L-alexa fluor 488 revealed an overlap of the nucleolin signal with that of the N6L-alexa fluor 488 (Fig. 4D), indicating that N6L translocates to the nucleolus. Similar observations were obtained with N6L-rhodamine validating these observations (data not shown). In addition, N6L translocation to the nucleolus was energy-dependent because it was inhibited when the cells were incubated at 4°C with 0.02% sodium azide to block active internalization (Fig. 4C). Taken together, these results are consistent with the translocation of N6L from the cell surface to the nucleolus. These data were reinforced by the observation carried out on living cells by using time-lapse imaging (Supplementary Movie, File N6L2.mp4). In addition, knockdown of nucleolin or nucleophosmin by siRNA strongly decreased N6L translocation from cell surface to nucleolus (Fig. 4E and F). This result provides strong evidence that nucleolin and nucleophosmin are involved in N6L trafficking.

N6L exhibits a proapoptotic activity *in vitro*

We used video microscopy to carry out direct analysis of the metabolism of the N6L pseudopeptide. MDA-MB 231 cells were incubated in the presence of N6L-alexa fluor 488 and analyzed for 14 hours by time-lapse video microscopy. Treated cells rapidly rounded and revealed morphologic features of characteristic apoptosis, such as cell shrinkage, cell membrane blebbing, and formation of apoptotic bodies (Fig. 5A and Supplementary Movie).

To validate these observations, apoptosis of N6L-treated cells was quantified by flow cytometry using Annexin V/PI and DIOC6 staining. N6L markedly increased Raji cell apoptosis in a concentration-dependent (Fig. 5B and C) and time-dependent manner (Fig. 5D). Similar data were obtained using MDA-MB 231 and MDA-MB 435 cells (Supplementary Table S2). To further confirm that N6L-induced cell death was due to apoptosis, we analyzed caspase-3/7 activation, which is considered

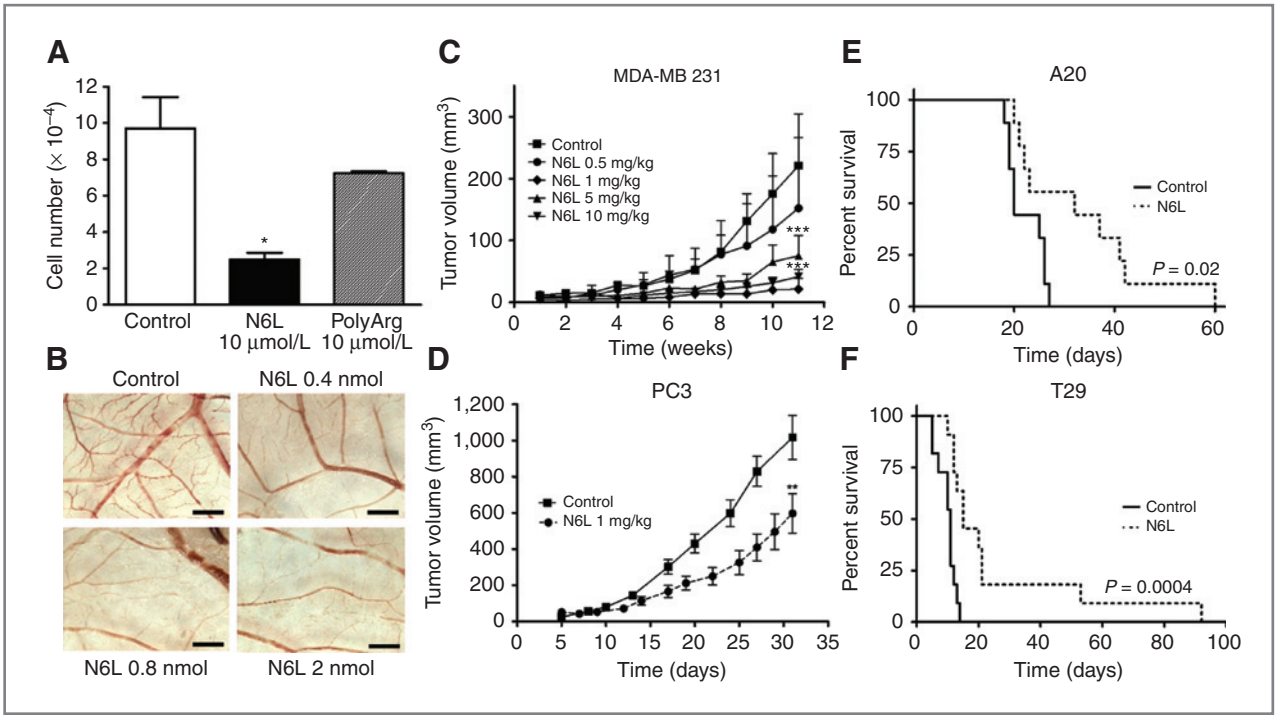

Figure 2. N6L treatment improves clinical features in angiogenesis and tumor models. A, inhibition of HUVEC cell growth by N6L. Cells were cultured for 3 days in the presence or absence of 10 μmol/L N6L or of PolyArg peptide used as the control. Cell growth was quantified by crystal violet staining. *, $P < 0.05$, statistically significant compared to control (Student *t* test). B, inhibition of *in vivo* angiogenesis by N6L in a chick CAM assay. The relative percentage inhibition ($P < 0.001$) of angiogenesis compared to the control was 25% in the presence of either 0.4 or 0.8 nmol N6L and 30% in the presence of 2 nmol N6L. Scale bars represent 1 mm. C, N6L inhibits MDA-MB 231 ectopic tumor growth in a dose-response manner, compared to the control (PBS-treated group) with 90% of inhibition at a dose of 1 mg/kg. D, N6L at 1 mg/kg inhibits human prostatic tumor (PC3) cell growth around 40% in nude mice. Mean tumor volume is indicated for each group. Bars ± SEM ($n = 6$ per group for MDA-MB 231 and $n = 10$ per group for PC3); **, $P < 0.01$; ***, $P < 0.001$ statistically significant compared to the control (Student *t* test). E and F, N6L improves survival of murine B (E) and T (F) lymphoma models compared to 0.9% NaCl-treated group ($n = 10$ per group). Comparison of survival duration was done using the Kaplan–Meier product-limit method, with analysis by the log rank test. Statistical significance was defined as $P < 0.05$.

to be a common hallmark of apoptosis. Raji cells were treated with concentrations of N6L ranging from 0 to 50 μmol/L for 48 hours and caspase-3 activity was determined in the cell lysate. N6L was found to induce caspase-3/7 activation in a dose-dependent manner. A 2-fold increase in caspase-3/7 activity compared with the basal level was observed in cells treated with 20 μmol/L N6L (Fig. 5E).

In vivo tumor targeting of N6L

Mice bearing MDA-MB 231 tumors were i.v. injected with 100 μg of N6L-alexa fluor 633 and subjected to fluorescence tracking in a bioimager. Images were collected every 2 minutes over the first 20 minutes, then every 24 hours. N6L-alexa fluor 633 revealed wide tissue distribution, including tumor tissue, immediately after injection, thus demonstrating the rapid addressing of the peptide due to efficient perfusion (Fig. 6A). A persistent signal in the tumor and in various other organs, including lung, kidney, liver, and brain, was observed. Postmortem collection of these tissues confirmed the retention of N6L-alexa fluor 633 24 hours postinjection. The signal intensity progressively decreased in all organs while increasing in the tumor mass until 48 hours postinjection, revealing the natural enrichment of the N6L pseudopeptide in tumors (Fig. 6B). Interestingly, persistent enrichment of N6L-alexa fluor 633 was also observed in the tumor mass in case of repeated injections (every day for 3 days; Fig. 6C). In addition, and as a control, we also monitored the distribution of N6L-alexa fluor 633 in mice without implanted tumor cells. In this case, we observed widespread distribution with most of the pseudopeptide being in lung, kidney, and liver, whereas no detectable signal was found in spleen and brain (Supplementary Fig. S2A and B). An additional control was carried out with the inactive N6L-alexa fluor 633 template in mice bearing tumors. A widespread distribution was also observed with no detectable fluorescence enrichment in the tumor mass (Supplementary Fig. S5).

N6L mediates caspase-dependent apoptosis *in vivo*

Sections of tumor xenografts from MDA-MB 231 cells treated or not with N6L were subjected to TUNEL staining (Fig. 5F). This staining causes a red fluorescence to appear that corresponds to a $5'PO_4$ DNA fragment cleaved by type I DNAse activated by caspase-3 and involved in self-execution apoptosis, as well as a green fluorescence that corresponds to an independently activated 5′-OH DNA fragment cleaved by type II DNAse caspase. Low red and green fluorescence was

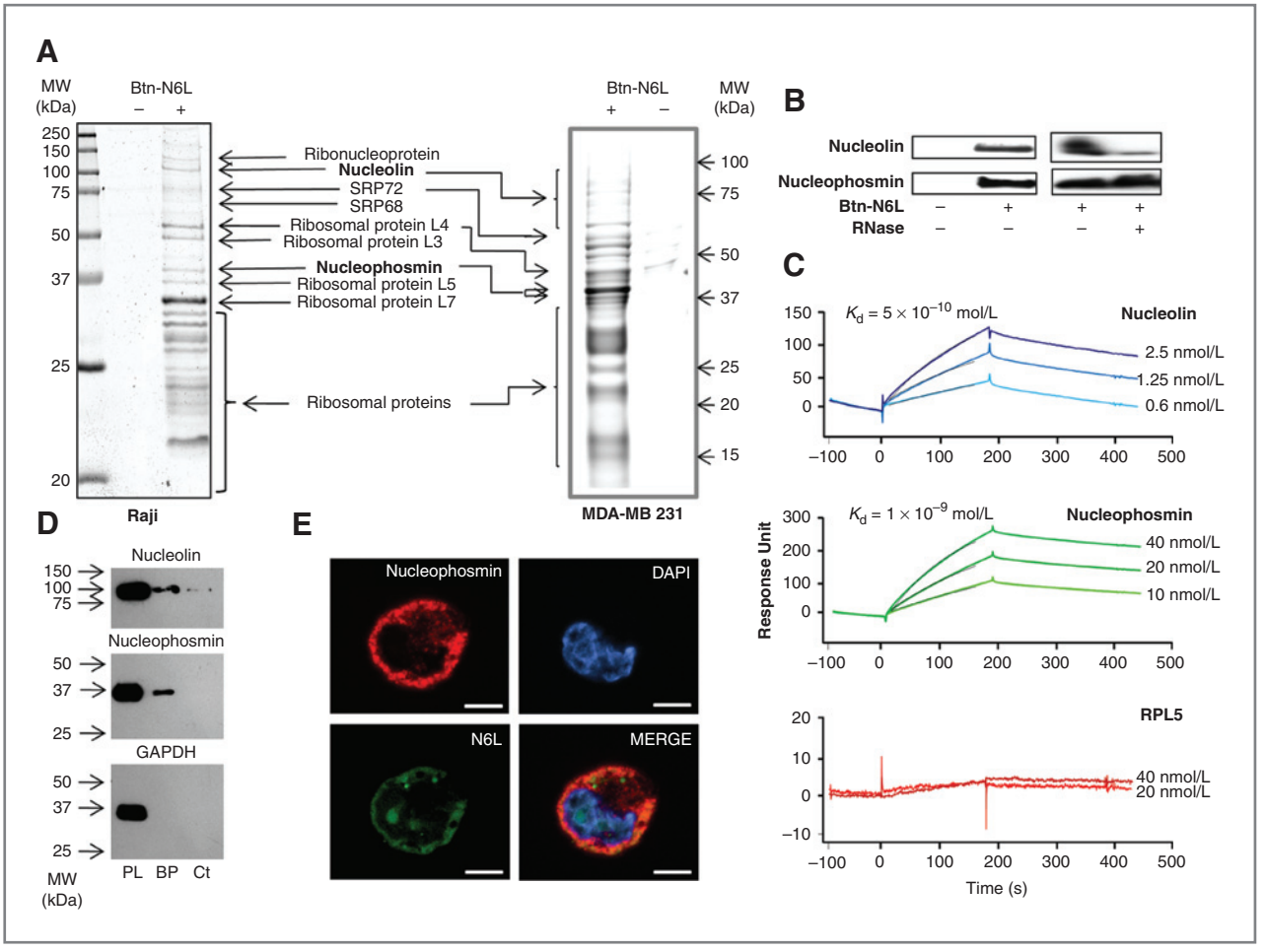

Figure 3. Identification of the molecular targets of N6L. A, biotin-labeled N6L binds to a nucleoproteic complex including nucleolin and nucleophosmin expressed on the surface of Raji or MDA-MB 231 cells. Affinity isolated proteins with biotin-labeled N6L (+) or without (–) were subjected to SDS-PAGE and revealed by colloidal blue for mass spectrometry identification. B, identification of nucleolin and nucleophosmin in isolated fraction was confirmed by immunoblot analysis. Pretreatment of cellular lysate without (–) or with (+) RNase A (100 μg/mL) was carried out to evaluate impact on identified interactions. C, direct binding of N6L to recombinant nucleolin, nucleophosmin, and ribosomal L5 protein used at different concentrations, as measured in surface plasmon resonance experiments. D, MDA-MB 231 cell-surface protein expression. Cell-surface proteins were labeled with biotin. Biotinylated proteins (BP) were purified on streptavidin beads and then subjected to SDS-PAGE, and the presence of nucleolin, nucleophosmin, and GAPDH was revealed by Western blot. Nonbiotinylated protein lysate (C_t) purified on streptavidin beads served as control for purification specificity. Normal protein lysate (PL) was used to observe the expected bands. E, colocalization of N6L and nucleophosmin on MDA-MB 231. Cells were fixed by PFA 4%, and N6L-alexa fluor 488 0.5 μmol/L was added as the primary antibody. Nucleophosmin was stained using antinucleophosmin (ab10530) primary antibody. The scale bars represent 5 μm.

observed in control tumors, indicating that the number of apoptotic cells was very low (relative score of 1,911 ± 487, $n = 5$). In N6L-treated tumors, strong red signals (relative score of 35,580 ± 8,553, $n = 5$)—but no green ones—were observed.

Comparison of the relative scores indicated that the inhibition of tumor growth in athymic mice by N6L occurred through the induction of caspase-dependent cell apoptosis ($P < 0.001$). Similar results were obtained in experiments carried out using xenograft PC-3 cells (Supplementary Fig. S3).

Discussion

The results presented in this study demonstrate the antitumor activity of a new multivalent pseudopeptide called N6L. Using an optical imaging system, this effect was validated *in vivo,* showing that N6L specifically targeted the tumor. These experiments were carried out in mice bearing MDA-MB 231 (Fig. 6A) or U373MG tumors (Supplementary Fig. S4). One of the major result of this study is the demonstration that N6L promotes apoptosis, as shown in both *in vitro* and *in vivo* experiments. Induction of apoptosis by N6L was directly observed by video microscopy in N6L-treated cells that exhibited abnormal cell morphology characteristic of apoptosis (28). Nucleolin has been identified as a Bcl-2 mRNA-stabilizing protein in the HL-60 human leukemia cell line (20, 29). More recently, it has been shown that the resistance of B-cell lymphocytic leukemias to apoptosis as a result of *Bcl-2* gene overexpression is related to stabilization of *Bcl-2* mRNA by

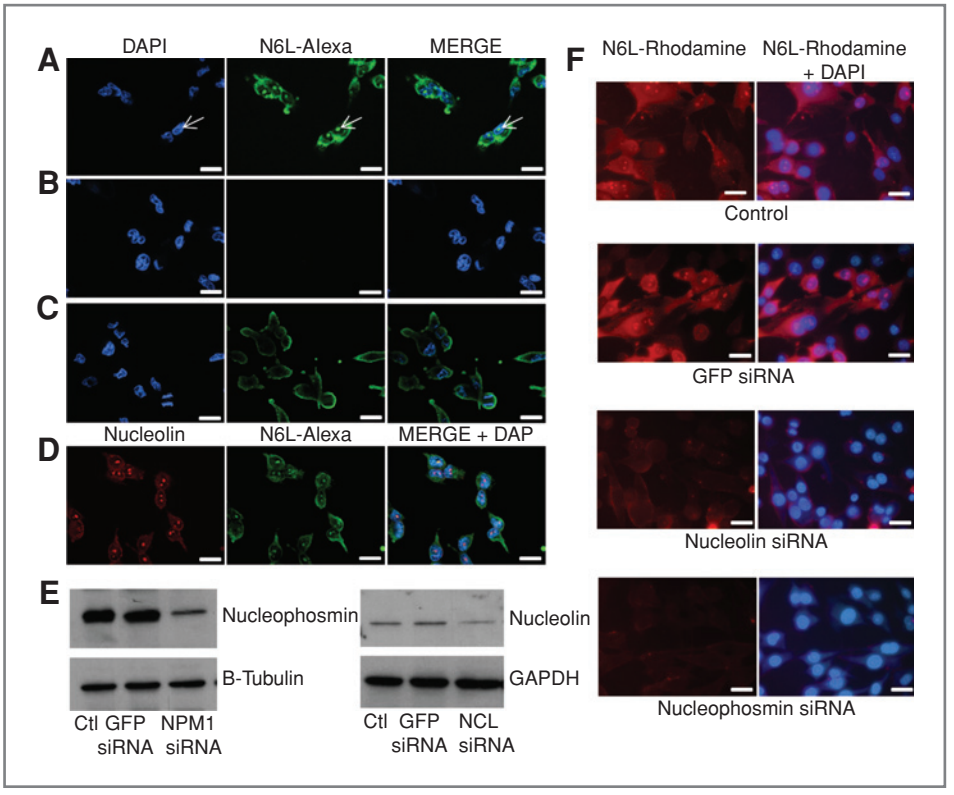

Figure 4. N6L is internalized in MDA-MB 231 cells to nucleolus at 37°C. A, MDA-MB 231 cells were incubated with 0.5 μmol/L N6L-alexa fluor 488 alone or (B), in the presence of 50 μmol/L N6L for 30 minutes at 37°C. Cells were then fixed with methanol and nuclei stained with 1 μg/mL of DAPI. C, MDA-MB 231 cells were incubated with 0.5 μmol/L N6L-alexa fluor 488 for 30 minutes at 4°C in the presence of 0.02% sodium azide and then fixed with methanol. Nuclei were stained with 1 μg/mL of DAPI. D, the nuclear structure stained by N6L-alexa fluor 488 is the nucleolus. Cells were incubated with N6L-alexa fluor 488 for 30 minutes at 37°C and then fixed with cold acetone. Nucleolin was stained by MS-3 primary antibody and the complex was revealed using an anti-mouse secondary antibody coupled to alexa fluor 568. MERGE represents N6L-alexa fluor 488, nucleolin, and nuclear staining by DAPI. The scale bars represent 20 μm. E, silencing efficiency of nucleophosmin (NPM1) and nucleolin (NCL) siRNA on MDA-MB 435 cells by Western blot. GFP siRNA was used as nontargeting control siRNA. F, translocation of N6L into the nucleus is inhibited by knockdown of nucleophosmin or nucleolin using siRNA. MDA-MB 435 cells were transfected for 48 hours. Then, 1 μmol/L of N6L was added for 10 minutes. Cells were washed twice with PBS and fixed with methanol. Fluorescence was observed using a fluorescent microscope. Scale bars represent 10 μm.

nucleolin (21). In addition, siRNA knockdown of nucleolin resulted in decreased *Bcl-2* mRNA stability and decreased levels of Bcl-2 protein in MCF-7 cells (30). Interestingly, several nucleolin ligands were shown to be involved in the induction of apoptosis. For example, the nucleolin-targeting aptamer AS1411 has been shown to induce apoptosis by interfering with the binding of nucleolin to *Bcl-2* mRNA (30). Similarly, antinucleolin antibody treatment destabilizes *Bcl-2* mRNA, leading to endothelial cell apoptosis (19). Endostatin, a 20-kDa polypeptide that is a potent inhibitor of angiogenesis and tumor growth (31), binds specifically cell-surface nucleolin (17). Study of the mechanism of action of endostatin on tumor growth has indicated that it induces apoptosis through activation of caspase-3 and a decrease in *Bcl-2* mRNA (32, 33). Taken together, these observations indicate that cell-surface nucleolin is highly involved in the apoptosis process, which is also supported by the present results showing that N6L is a proapoptotic molecule able to induce tumor cell death.

Although cell-surface nucleolin is a good candidate for N6L-mediated apoptosis induction, we cannot exclude that other N6L-binding proteins and/or nucleolin-binding proteins could be involved and might play a role in this process. To test this hypothesis, a series of affinity isolation experiments were carried out. As expected, nucleolin was identified, but also several other proteins, including ribosomal proteins and signal recognition particle proteins involved in the packing and transport of RNA, as well as nucleophosmin. Because all the proteins identified in this experiment belong to a protein family that shares the common property of being able to bind nucleolin, we can assume that most of these affinity-isolated proteins are associated in a macromolecular complex that includes cell-surface nucleolin (34). Among these proteins, nucleophosmin is an important target for cancer suppression and is involved in apoptosis regulation. Studies using a peptide derived from Rev protein, which binds nucleophosmin, suppressed tumor growth through apoptosis by upregulating the transcriptional activity of p53. Recently, NSC348884, a pharmacophore that targets nucleophosmin, has been shown to inhibit the proliferation of various cancer cell lines through the induction of apoptosis (35). Likewise, it has been shown that

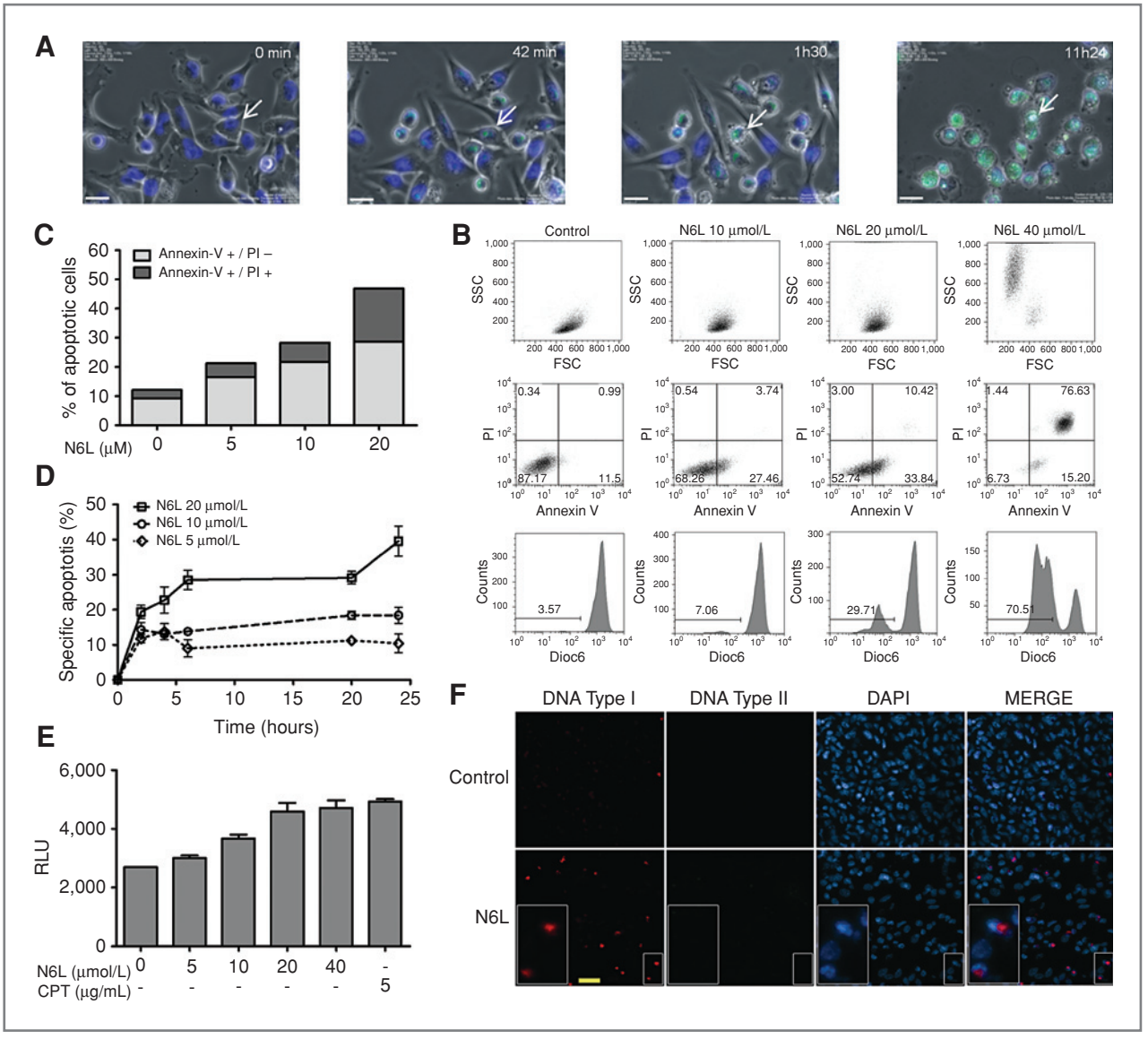

Figure 5. N6L induces apoptosis in treated tumors cells. A, analysis of the biological effect of N6L by time-lapse video-microscopy analysis. Ten μmol/L of N6L alexa-fluor 488 was added to MDA-MB 231 cells. Nuclei were stained with Hoechst reagent. Pictures were taken with a time-lapse system every 10 minutes for 14 hours. Arrows indicate the evolution of one cell. Scale bars represent 10 μm. B, N6L (0–40 μmol/L for 16 hours) induces a decrease of mitochondrial Δm in Raji cells, measured by the reduction of DIOC6 dye uptake, early apoptosis measured by Annexin V- allophycocyanin-labeling, and morphologic changes relative to apoptosis shown in an SSC/FSC plot obtained by flow cytometry. C, percentage of early (Annexin V+/PI−) and late apoptotic cells (Annexin V+/PI+) measured in flow cytometry during N6L-induced apoptosis of Raji cells after 16 hours of treatment. D, time-course of apoptosis induction of Raji cells by N6L peptide at increasing concentrations. Results are expressed as percentage of specific apoptosis according to the following formula: percentage specific apoptosis = [(percentage of apoptotic treated cells – percentage of apoptotic control cells) × 100]/(100 – percentage of apoptotic control cells). E, caspase-3/7 activity in Raji cells treated with different concentrations of N6L or by camptothecin as a positive control for 24 hours; RLU, relative light units. F, N6L induces caspase-dependant apoptosis *in vivo* in MDA-MB 231 tumors. Red signal corresponds to type I DNAse activation-dependent on caspase-3 activation. Green signal corresponds to type II DNAse activation-independent of caspase activation. Scale bar represents 50 μm.

both nucleophosmin and nucleolin, which are overexpressed at the cell surface of tumor cells compared with normal resting cells (36), regulate K-Ras plasma membrane interactions and mitogen-activated protein kinase signal transduction. Analysis of the binding domains involved in these interactions revealed that nucleophosmin binds to the basic domain of K-Ras. This stretch of basic residues interacts with the N-terminal globular domain of nucleophosmin, which has been shown to be involved in nucleophosmin pentamer formation and chaperone activity. It is noteworthy that molecules that interact with the N-terminal domain of nucleophosmin, such as the Rev peptide (37) or the small molecule NSC 348884 (35), disrupt

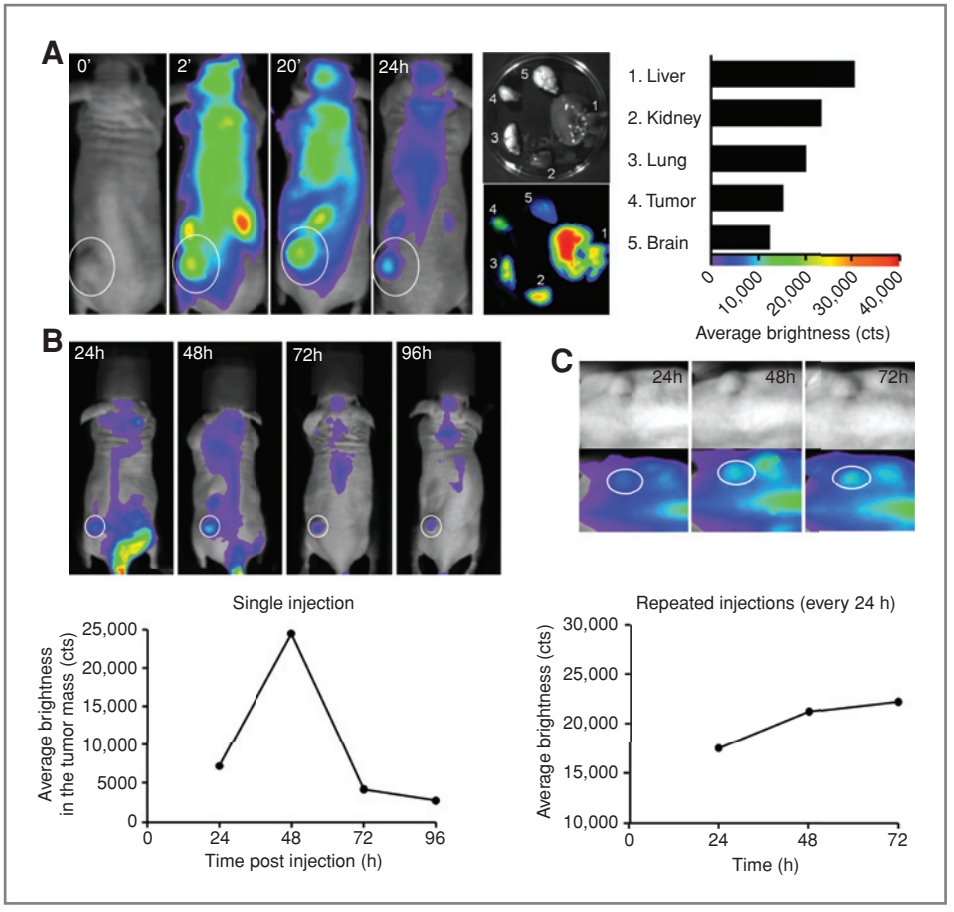

Figure 6. *In vivo* imaging of N6L distribution in mice bearing MDA-MB 231 tumors. A, fluorescence was monitored for 24 hours using the NightOwl bioimager after injection of 100 μg N6L-alexa fluor 633 in PBS into mice bearing MDA-MB 231 tumor. At the end of the experiment (24 hours), organs were collected and fluorescence was measured in the isolated organs. B, enrichment of N6L in tumors. Representative fluorescence images in mice imaged 24 to 48 hours after injection of 100 μg of N6L-alexa fluor 633 into the tail vein. The higher fluorescence level is observed in tumor (white circle) 48 hours after injection. C, enrichment of N6L in tumors after repeated injections (every 24 hours) of 100 μg of N6L-alexa fluor 633 to mice bearing MDA-MB 231 tumors.

nucleophosmin oligomer formation and induce apoptosis. From this set of results, we can hypothesize that N6L, which is a pseudopeptide rich in Lys and Arg residues and displays high affinity for nucleophosmin, disrupts its oligomerization and/or the formation of complexes between nucleolin, nucleophosmin, and oncoproteins. Another piece of data presented herein concerns cellular trafficking of N6L to the tumor cell nucleolus. Following its binding to cell-surface nucleoproteins, N6L is internalized and rapidly concentrates in the nucleolus. This result was obtained using fluorescent video-microscopy analysis on live cells and was further confirmed by histologic studies using N6L tagged with fluorescent molecules. The mechanism by which N6L is translocated to the nucleolus remains unknown and is currently under investigation. However, it is tempting to speculate that N6L could be translocated to the nucleolus through its interaction with nucleoproteins. These results are supported by our experiments on N6L trafficking on nucleolin and nucleophosmin knockdown cells. Nevertheless, the relationship between localization of N6L in the nucleolus and its biological effect has not yet been established and will be explored in further studies.

Viewed collectively, the data presented in this article indicate that the multivalent pseudopeptide N6L induces apoptosis of tumor cells, which could therefore constitute a possible mechanism by which N6L demonstrates antitumor activity. Both nucleolin and nucleophosmin are multifunctional pleiotropic proteins involved in several important cell processes, suggesting that the antiproliferative effect of N6L could be mediated by several different mechanisms of action that remain to be identified.

Disclosure of Potential Conflicts of Interest

No potential conflicts of interest were disclosed.

Acknowledgments

The authors thank M. Duval and S. Besse for their valuable assistance, G. Courty for the video editing, and Dr P. Kastner (IGBMC, Strasbourg) for the gift of T29 cells.

Grant Support

This research was funded by the CNRS, the Région Alsace, La Ligue contre le Cancer, and the Ministère de l'Enseignement Supérieur et de la Recherche.

The costs of publication of this article were defrayed in part by the payment of page charges. This article must therefore be hereby marked *advertisement* in accordance with 18 U.S.C. Section 1734 solely to indicate this fact.

Received September 23, 2010; revised February 24, 2011; accepted March 9, 2011; published OnlineFirst March 17, 2011.

References

1. Christian S, Pilch J, Akerman ME, Porkka K, Laakkonen P, Ruoslahti E. Nucleolin expressed at the cell surface is a marker of endothelial cells in angiogenic blood vessels. J Cell Biol 2003;163:871–8.
2. Ginisty H, Sicard H, Roger B, Bouvet P. Structure and functions of nucleolin. J Cell Sci 1999;112:761–72.
3. Hovanessian AG, Puvion-Dutilleul F, Nisole S, Svab J, Perret E, Deng JS, et al. The cell-surface-expressed nucleolin is associated with the actin cytoskeleton. Exp Cell Res 2000;261:312–28.
4. Srivastava M, Pollard HB. Molecular dissection of nucleolin's role in growth and cell proliferation: new insights. FASEB J 1999;13:1911–22.
5. Di Segni A, Farin K, Pinkas-Kramarski R. Identification of nucleolin as new ErbB receptors- interacting protein. PLoS One 2008;3:e2310.
6. Said EA, Courty J, Svab J, Delbe J, Krust B, Hovanessian AG. Pleiotrophin inhibits HIV infection by binding the cell surface-expressed nucleolin. FEBS J 2005;272:4646–59.
7. Said EA, Krust B, Nisole S, Svab J, Briand JP, Hovanessian AG. The anti-HIV cytokine midkine binds the cell surface-expressed nucleolin as a low affinity receptor. J Biol Chem 2002;277:37492–502.
8. Tate A, Isotani S, Bradley MJ, Sikes RA, Davis R, Chung LW, et al. Met-Independent Hepatocyte Growth Factor-mediated regulation of cell adhesion in human prostate cancer cells. BMC Cancer 2006;6:197.
9. Dumler I, Stepanova V, Jerke U, Mayboroda OA, Vogel F, Bouvet P, et al. Urokinase-induced mitogenesis is mediated by casein kinase 2 and nucleolin. Curr Biol 1999;9:1468–76.
10. Stepanova V, Lebedeva T, Kuo A, Yarovoi S, Tkachuk S, Zaitsev S, et al. Nuclear translocation of urokinase-type plasminogen activator. Blood 2008;112:100–10.
11. Harms G, Kraft R, Grelle G, Volz B, Dernedde J, Tauber R. Identification of nucleolin as a new L-selectin ligand. Biochem J 2001;360:531–8.
12. Larrucea S, González-Rubio C, Cambronero R, Ballou B, Bonay P, López-Granados E, et al. Cellular adhesion mediated by factor J, a complement inhibitor. Evidence for nucleolin involvement. J Biol Chem 1998;273:31718–25.
13. Reyes-Reyes EM, Akiyama SK. Cell-surface nucleolin is a signal transducing P-selectin binding protein for human colon carcinoma cells. Exp Cell Res 2008;314:2212–23.
14. Turck N, Lefebvre O, Gross I, Gendry P, Kedinger M, Simon-Assmann P, et al. Effect of laminin-1 on intestinal cell differentiation involves inhibition of nuclear nucleolin. J Cell Physiol 2006;206:545–55.
15. Bates PJ, Laber DA, Miller DM, Thomas SD, Trent JO. Discovery and development of the G-rich oligonucleotide AS1411 as a novel treatment for cancer. Exp Mol Pathol 2009;86:151–64.
16. Drecoll E, Gaertner FC, Miederer M, Blechert B, Vallon M, Müller JM, et al. Treatment of peritoneal carcinomatosis by targeted delivery of the radio-labeled tumor homing peptide bi-DTPA-[F3]2 into the nucleus of tumor cells. PLoS One 2009;4:e5715.
17. Shi H, Huang Y, Zhou H, Song X, Yuan S, Fu Y, et al. Nucleolin is a receptor that mediates antiangiogenic and antitumor activity of endostatin. Blood 2007;110:2899–906.
18. Destouches D, El Khoury D, Hamma-Kourbali Y, Krust B, Albanese P, Katsoris P, et al. Suppression of tumor growth and angiogenesis by a specific antagonist of the cell-surface expressed nucleolin. PLoS One 2008;3:e2518.
19. Fogal V, Sugahara KN, Ruoslahti E, Christian S. Cell surface nucleolin antagonist causes endothelial cell apoptosis and normalization of tumor vasculature. Angiogenesis 2009;12:91–100.
20. Otake Y, Sengupta TK, Bandyopadhyay S, Spicer EK, Fernandes DJ. Retinoid-induced apoptosis in HL-60 cells is associated with nucleolin down-regulation and destabilization of Bcl-2 mRNA. Mol Pharmacol 2005;67:319–26.
21. Otake Y, Soundararajan S, Sengupta TK, Kio EA, Smith JC, Pineda-Roman M, et al. Overexpression of nucleolin in chronic lymphocytic leukemia cells induces stabilization of bcl2 mRNA. Blood 2007;109:3069–75.
22. Takagi M, Absalon MJ, McLure KG, Kastan MB. Regulation of p 53 translation and induction after DNA damage by ribosomal protein L26 and nucleolin. Cell 2005;123:49–63.
23. Ugrinova I, Monier K, Ivaldi C, Thiry M, Storck S, Mongelard F, et al. Inactivation of nucleolin leads to nucleolar disruption, cell cycle arrest and defects in centrosome duplication. BMC Mol Biol 2007;8:66.
24. Grinstein E, Shan Y, Karawajew L, Snijders PJ, Meijer CJ, Royer HD, et al. Cell cycle-controlled interaction of nucleolin with the retinoblastoma protein and cancerous cell transformation. J Biol Chem 2006;281:22223–35.
25. Blondet B, Carpentier G, Ferry A, Courty J. Exogenous pleiotrophin applied to lesioned nerve impairs muscle reinnervation. Neurochem Res 2006;31:907–13.
26. Celik I, Sürücü O, Dietz C, Heymach JV, Force J, Höschele I, et al. Therapeutic efficacy of endostatin exhibits a biphasic dose-response curve. Cancer Res 2005; 65:11044–50.
27. Page N, Schall N, Strub JM, Quinternet M, Chaloin O, Decossas M, et al. The spliceosomal phosphopeptide P140 controls the lupus disease by interacting with the HSC70 protein and via a mechanism mediated by gammadelta T cells. PLoS One 2009;4:e5273.
28. Majno G, Joris IApoptosis, oncosis, and necrosis. An overview of cell death. Am J Pathol 1995;146:3–15.
29. Sengupta TK, Bandyopadhyay S, Fernandes DJ, Spicer EK. Identification of nucleolin as an AU-rich element binding protein involved in bcl-2 mRNA stabilization. J Biol Chem 2004;279:10855–63.
30. Soundararajan S, Chen W, Spicer EK, Courtenay-Luck N, Fernandes DJ. The nucleolin targeting aptamer AS1411 destabilizes Bcl-2 messenger RNA in human breast cancer cells. Cancer Res 2008;68:2358–65.
31. O'Reilly MS, Boehm T, Shing Y, Fukai N, Vasios G, Lane WS, et al. Endostatin: an endogenous inhibitor of angiogenesis and tumor growth. Cell 1997;88:277–85.
32. Dhanabal M, Ramchandran R, Waterman MJ, Lu H, Knebelmann B, Segal M, et al. Endostatin induces endothelial cell apoptosis. J Biol Chem 1999;274:11721–6.
33. Ling Y, Lu N, Gao Y, Chen Y, Wang S, Yang Y, et al. Endostar induces apoptotic effects in HUVECs through activation of caspase-3 and decrease of Bcl-2. Anticancer Res 2009;29:411–7.
34. Inder KL, Lau C, Loo D, Chaudhary N, Goodall A, Martin S, et al. Nucleophosmin and nucleolin regulate K-Ras plasma membrane interactions and MAPK signal transduction. J Biol Chem 2009;284:28410–9.
35. Qi W, Shakalya K, Stejskal A, Goldman A, Beeck S, Cooke L, et al. NSC348884, a nucleophosmin inhibitor disrupts oligomer formation and induces apoptosis in human cancer cells. Oncogene 2008;27:4210–20.
36. Feuerstein N, Chan PK, Mond JJ. Identification of numatrin, the nuclear matrix protein associated with induction of mitogenesis, as the nucleolar protein B23. Implication for the role of the nucleolus in early transduction of mitogenic signals. J Biol Chem 1988;263:10608–12.
37. Chan HJ, Weng JJ, Yung BY. Nucleophosmin/B23-binding peptide inhibits tumor growth and up-regulates transcriptional activity of p53. Biochem Biophys Res Commun 2005;333:396–403.